University of Groningen

Influence of capping layers on the crystallization of doped SbxTe fast-growth phase-change films

Pandian, Ramanathaswamy; Kooi, Bart J.; De Hosson, Jeff Th. M.; Pauza, Andrew

Published in:
Journal of Applied Physics

DOI:
10.1063/1.2401308

IMPORTANT NOTE: You are advised to consult the publisher's version (publisher's PDF) if you wish to cite from it. Please check the document version below.

Document Version
Publisher's PDF, also known as Version of record

Publication date:
2006

Link to publication in University of Groningen/UMCG research database

Citation for published version (APA):
Pandian, R., Kooi, B. J., De Hosson, J. T. M., & Pauza, A. (2006). Influence of capping layers on the crystallization of doped SbxTe fast-growth phase-change films. *Journal of Applied Physics*, *100*(12), 123511-1 - 123511-9. [123511]. https://doi.org/10.1063/1.2401308

Copyright
Other than for strictly personal use, it is not permitted to download or to forward/distribute the text or part of it without the consent of the author(s) and/or copyright holder(s), unless the work is under an open content license (like Creative Commons).

The publication may also be distributed here under the terms of Article 25fa of the Dutch Copyright Act, indicated by the "Taverne" license. More information can be found on the University of Groningen website: https://www.rug.nl/library/open-access/self-archiving-pure/taverne-amendment.

Take-down policy
If you believe that this document breaches copyright please contact us providing details, and we will remove access to the work immediately and investigate your claim.

Downloaded from the University of Groningen/UMCG research database (Pure): http://www.rug.nl/research/portal. For technical reasons the number of authors shown on this cover page is limited to 10 maximum.

Influence of capping layers on the crystallization of doped Sb_xTe fast-growth phase-change films

Ramanathaswamy Pandian, Bart J. Kooi,[a] and Jeff Th. M. De Hosson
Department of Applied Physics, Materials Science Center, and Netherlands Institute for Metals Research, University of Groningen, Nijenborgh 4, 9747 AG Groningen, the Netherlands

Andrew Pauza
Plasmon Data Systems Ltd., Whiting Way, Melbourn Royston, Hertsfordshire SG8 6EN, United Kingdom

(Received 28 April 2006; accepted 7 October 2006; published online 22 December 2006)

Isothermal crystallization of doped Sb_xTe fast-growth phase-change films, with and without capping layers, was investigated using transmission electron microscopy, which provided direct and quantitative information on nucleation and growth processes separately. Two types of amorphous dielectric layers, $ZnS-SiO_2$ and GeCrN, were used for sandwiching the Sb_xTe films to form typical trilayer stacks, which are the active part in applications. The nucleation and growth parameters of Sb_xTe films were found to be influenced by the dielectric capping layers. The crystal growth rate is temperature dependent and it reduces when the film is sandwiched between the dielectric layers. The reduction in growth rate differs with the capping layer type. The capping layer influence on the growth rate is pronounced at lower temperatures ~160 °C, but tends to vanish at higher temperatures ~200 °C. The activation energy for crystal growth is 2.4±0.3 eV for an uncapped film and it increases ~40% when the capping layers, GeCrN or $ZnS-SiO_2$, are added. A temperature and time dependent nucleation rate is found and it is accelerated ~1.7 times by GeCrN layers, whereas it is retarded ~5 times by $ZnS-SiO_2$ layers. The activation energy for crystal nucleation is 6.1±0.4 eV for an uncapped film and it is not noticeably altered by the capping layers. These variations observed in the crystallization kinetics are attributed to variations in interface energy between the phase-change film and the capping layers or vacuum and the confinement effect by the capping layers on the phase-change film. © *2006 American Institute of Physics*.
[DOI: 10.1063/1.2401308]

I. INTRODUCTION

Chalcogenide based materials are currently used in phase-change optical disks [rewritable formats of the compact disk (CD), digital versatile disk (DVD), Blu-ray disk, and high-density DVD (HD-DVD)] and also tested for electrical nonvolatile memory devices such as "phase-change random access memory" (PRAM) or "Ovonic unified memory" (OUM).[1–10] In both the optical and electrical phase-change data storage methods, data are written by locally melt quenching the crystalline phase-change film into an amorphous state using an optical (laser) or electrical pulse. The written amorphous bit can be read due to its large optical (reflectivity) or electrical (resistivity) contrast with the surrounding crystalline background. Erasing data involves heating the amorphous bit to temperatures between the crystallization and melting points and allowing it to recrystallize. When considering the data transfer rate, amorphization is relatively a much faster process than crystallization, and hence crystallization becomes the rate limiting process especially during direct overwriting. Thus, understanding the kinetics of crystallization is of great importance for developing high-speed phase-change recording materials.

Several types of materials for phase-change recording can be recognized.[11–14] Among them doped alloys derived from "eutectic" Sb_xTe, showing a growth-dominant crystallization behavior, appear the most obvious choice for both high data transfer rate and high-density recording.[15–20] These materials are currently used in optical disk formats including DVD+RW, DVD-RW, Blu-ray disk,[21] and HD-DVD,[22] and are also proposed for the line concept PRAM.[23] A good trade-off between crystallization speed and data retention time is also expected in these materials, as they appear to have a high activation energy for crystallization.

In phase-change optical disks, the active layer is actually sandwiched between dielectric layers, which are transparent to semiconductor laser wavelength. Similar stacks are also relevant for PRAM, in particular, for the recently proposed line concept.[23] Dielectric layer protection is necessary due to several reasons, particularly to control the fluidization and vaporization of the phase-change material during the recording process and to protect the phase-change layer from thermal stress cycle during repetitious overwriting.[24] Consequently, several properties of the phase-change layer including crystallization are significantly altered by the capping layers.[24–28] Therefore, the combination of the phase-change film and capping layers has to be considered, and improving understanding of the influence of capping layers on the crystallization kinetics of the phase-change film becomes vital in order to optimize the disk characteristics.

Ohshima[25] previously analyzed the influence of various dielectric capping layers on the crystallization of $Ge_1Sb_2Te_4$

[a]Author to whom correspondence should be addressed; electronic mail: b.j.kooi@rug.nl

 © 2006 American Institute of Physics

Downloaded 09 Feb 2007 to 129.125.25.39. Redistribution subject to AIP license or copyright, see http://jap.aip.org/jap/copyright.jsp

thin films based on transmittance-change measurements. However, transmittance measurements or other techniques[26–33] generally used, such as differential scanning calorimetry, x-ray diffraction, electrical (resistance) measurements, and reflectance measurements, provide information *only* on the overall crystallization process, that is actually an interplay of both nucleation and growth processes. In contrast, transmission electron microscopy (TEM) is capable of providing separate information on nucleation and growth parameters. Ruitenberg *et al.*[34] already performed isothermal crystallization studies using *in situ* TEM and determined the individual nucleation and growth parameters for the crystallization of nucleation-dominant-type $Ge_2Sb_2Te_5$ thin films sandwiched between Si_3N_4 dielectric layers. However, there are some inconsistencies between their listed nucleation and growth parameters and the (fitted) results predicted from the corresponding figures. Direct observations on nucleation and growth rates and the effects of the capping layers on these rates have not been reported yet for the so-called fast-growth-type phase-change materials. In this work, we quantitatively determine both the nucleation and growth parameters of doped Sb_xTe amorphous films and study the influence of two types of dielectric capping layers, namely, GeCrN and $ZnS-SiO_2$, using TEM with *in situ* annealing experiments. During the experiments, we have explicitly excluded the effect the electron beam of the TEM has on the nucleation and growth rates we observed in our previous works.[35–37] This is a first major difference of the present work with the work we presented in Ref. 37. Other important differences are as follows: In Ref. 37 nucleation rates were not obtained, but are reported here. In Ref. 37 samples with various Sb/Te ratios were grown by sputtering from multiple targets on silicon nitride membranes. Here, a single fixed Sb/Te ratio is used for all samples, where the films were obtained by sputtering from a single target on carbon coated copper grids. These latter substrates exhibit a better heat conduction than the former, which is important for the measurement strategy we adopted in the present work as will be explained in the next section.

II. EXPERIMENT

Two types of Sb_xTe films, named as single-layer film and sandwiched film, were prepared for the TEM experiments and the structures of the films are shown in Fig. 1. In the single-layer film structure [see Fig. 1(a)], an amorphous phase-change layer is deposited on a carbon coated copper grid (300 mesh). In the sandwiched film structure [see Fig. 1(b)], the phase-change layer is sandwiched between two amorphous dielectric layers and this trilayer stack is deposited on the carbon coated Cu grid. A constant dopant level (~8 at. % of Ge+In) was maintained with a fixed value for the Sb/Te ratio x in between 3.1 and 3.5 in the phase-change layer. The dielectric capping layers were composed of either 80 at. % ZnS-20 at. % SiO_2 ($ZnS-SiO_2$) or GeCrN. dc and rf magnetron sputtering techniques were used to deposit the phase-change and dielectric layers, respectively. The samples are stored in vacuum to prevent possible oxidation. However,

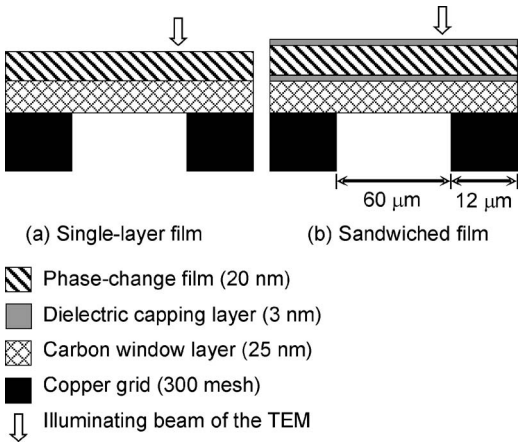

FIG. 1. Structures around the Sb_xTe films used for TEM experiments.

the uncapped samples can become oxidized to a small extent when they are transferred through air to the vacuum system of the TEM.

The samples were isothermally annealed at various temperatures between 160 and 185 °C inside a JEOL 2010F TEM operating at an accelerating voltage of 200 kV. A Gatan 652 double tilt heating holder with a 901 Smartset hot stage controller controls the sample temperature. A proportional integral derivative (PID) controller equipped with the furnace controls the temperature within ±0.5 °C accuracy and provides a fast ramp rate to attain the set-point temperature without any overshoot. However, the measured temperature is the furnace temperature, not the actual film temperature, which is expected to be slightly lower than the measured value and will show a time lag. To minimize this temperature difference and time lag, substrates with relatively good thermal conductance are desirable. Therefore, carbon coated copper grids were used in these experiments, instead of Si substrates (with a silicon nitride membrane on top) used in our previous works.[35–37] Moreover, for measurements, we choose areas as close as possible to the grid edges where a physical contact with the furnace is made and close to the grid bars as well in order to maximally reduce the temperature gradient.

Our previous works[35–37] showed that the crystallization of the phase-change film is sensitive to irradiation by the electron beam of the TEM; i.e., nucleation and growth rates increased. A detailed investigation of the influence of electron beam on the crystal growth is subject of a separate publication.[38] In order to entirely avoid such an influence in the present experiments, crystallization was carried out without electron beam exposure for fixed time intervals at elevated temperature. After each interval, the sample is cooled to nearly room temperature (below 30 °C) for TEM measurements, i.e., the measurements of nucleation and growth were made in discrete heating and cooling steps unlike in our previous studies,[35,36] where it was done in a more or less continuous manner. Using this procedure, it was important to switch from the silicon nitride membranes to the carbon coated copper grids with their better thermal conductance.

Nucleation and growth of crystals were monitored in bright-field mode of the TEM on a fluorescent screen and the

Downloaded 09 Feb 2007 to 129.125.25.39. Redistribution subject to AIP license or copyright, see http://jap.aip.org/jap/copyright.jsp

images were digitally recorded using a charge-coupled device (CCD) camera. A magnification of 40 000×, corresponding to 10.4 μm^2 field of view on the camera, turned out to be most suitable to determine the nucleation and growth parameters. It means that this magnification is high enough to follow the growth of individual crystal nuclei and at the same time it is low enough to count a substantial number of nuclei. However, to perform a more accurate and representative measurement on nucleation and growth for the entire sample, we monitored the crystallization within six to ten different areas on the sample. Sufficient statistics on nucleation is obtained by considering a combination of the individually monitored areas. The crystal radius is precisely measured by averaging the radii of more than six crystals monitored within the different sample areas. During each isothermal annealing, the number of crystal nuclei, the crystal radii, and the crystallized area fraction were measured as a function of time.

III. RESULTS

A. Growth properties

An example for the formation and growth of Sb_xTe crystals in an amorphous surrounding during crystallization is shown in Fig. 2. These TEM images hold for a $ZnS-SiO_2$ capped Sb_xTe film annealed at 180 °C. The crystals nucleate after a certain incubation time and grow nearly isotropically by maintaining their circular shape. The radius of the crystal increases more or less linearly with time, i.e., the crystal growth rate is (nearly) constant during isothermal annealing, implying an interface-controlled growth mechanism. Figure 3 shows the increase of the average crystal radius (r) as a function of time (t) at various annealing temperatures in uncapped Sb_xTe films as an example. The slope of the (r vs t) straight-line fit corresponds to the crystal growth rate that strongly increases with the annealing temperature (see Fig. 3). Careful analysis shows that the growth velocity is actually not a constant at each temperature, but is slightly increasing with time. This effect of an increasing growth velocity with time was also observed in our previous work and we attributed it to (a) relaxation process(es).[37] In the following we will disregard this effect, but we will address it in Ref. 38 where also the influence of electron beam of the TEM (that is now absent for the present measurements) on the growth velocity is analyzed in detail.

The temperature (T) dependence of the crystal growth rate (V_g) is adequately represented by the following Arrhenius-type equation:

$$V_g(T) = C_g \exp\left(\frac{-E_g}{k_B T}\right), \tag{1}$$

where E_g is the activation energy for crystal growth, C_g is the preexponential constant, and k_B is the Boltzmann constant. According to Eq. (1), plotting $\ln(V_g)$ against $1/T$ should provide a straight line. The slope of the line yields E_g, while the intercept represents $\ln(C_g)$. Arrhenius-type plots based on the measured crystal growth rates at various annealing temperatures for the capped and uncapped samples are shown in Fig. 4. This figure clearly shows that sandwiching the phase-change film between $ZnS-SiO_2$ or GeCrN layers leads to a reduction in growth rate. Variation in growth rate between the capped and uncapped film is larger at lower temperatures (~160 °C) compared to that at higher temperatures (~185 °C). Quantitative measurements reveal that the growth rate is reduced ~7 and 5 times by $ZnS-SiO_2$ and

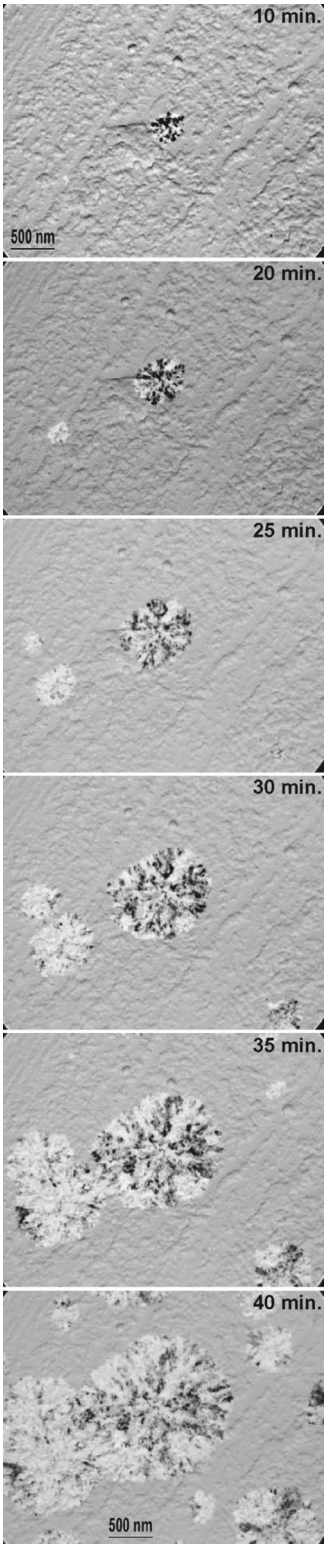

FIG. 2. Bright-field TEM images showing the nucleation and growth of crystals as a function of time during an isothermal crystallization of a Sb_xTe film sandwiched between $ZnS-SiO_2$ layers at 180 °C.

Downloaded 09 Feb 2007 to 129.125.25.39. Redistribution subject to AIP license or copyright, see http://jap.aip.org/jap/copyright.jsp

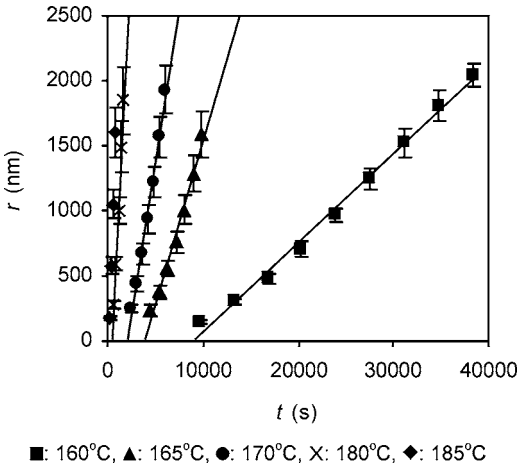

FIG. 3. Average crystal radius (r) as a function of time (t) during isothermal annealing of single-layer Sb_xTe films at various temperatures indicated.

GeCrN layers, respectively, at ~160 °C. This is a huge effect; however at ~185 °C, the growth rate is lowered only ~2 and 1.5 times by $ZnS-SiO_2$ and GeCrN layers, respectively. Hence, the influence of capping layers on growth rate reduces with increasing temperature and probably vanishes at higher temperatures (~200 °C).

The growth parameters E_g and $\ln(C_g)$ determined from the $\ln(V_g)$ vs $1/T$ linear fit (see Fig. 4) are listed in Table I for uncapped and capped samples. The activation energy for crystal growth of an uncapped Sb_xTe film is 2.4±0.3 eV and increases to 3.3±0.3 and 3.4±0.6 eV when the film is capped with GeCrN and $ZnS-SiO_2$ layers, respectively. These results show that the activation energy for crystal growth of Sb_xTe films is strongly influenced by the capping layers and the variation in activation energy (~40%) is not considerably dependent on the capping material type.

The activation energy for crystal growth of the uncapped Sb_xTe film is in good agreement with the one we reported[36] for e-beam evaporated (5 at. %) Ge-doped $Sb_{3.6}Te$ films (2.37±0.15 eV), and is also nearly identical to the activation energies found for the (uncapped) *nucleation-dominant* Ge–Sb–Te films [E_g=2.35±0.05 eV for $Ge_2Sb_2Te_5$ on Si (Ref. 39) and 2.4±0.3 eV for $Ge_2Sb_2Te_5$ on SiO_2 (Ref. 40)]. Ruitenberg *et al.*[34] reported E_g of 1.6±0.6 eV for a $Ge_2Sb_2Te_5$ film sandwiched between Si_3N_4 layers. This value is rather low compared to the activation energies of the

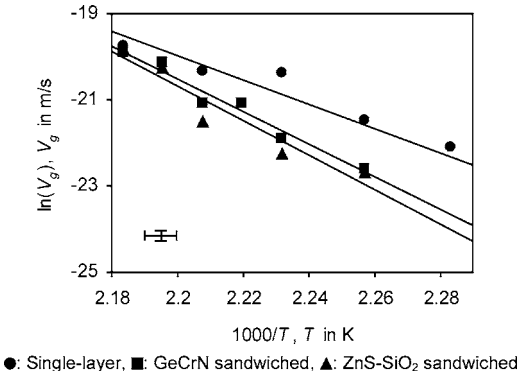

FIG. 4. Arrhenius plots of the growth rate (V_g) as a function of the annealing temperature (T) for the three types of capped Sb_xTe films.

TABLE I. Growth parameters E_g and $\ln(C_g)$ for the single-layer and sandwiched Sb_xTe films.

Sample	E_g (eV)	$\ln(C_g)$; C_g in m/s
Single-layer	2.4±0.3	42±8
GeCrN sandwiched	3.3±0.3	63±8
$ZnS-SiO_2$ sandwiched	3.4±0.6	67±16

sandwiched Sb_xTe films (E_g>3 eV) listed in Table I. From an application point of view, a higher E_g (as exhibited in our sandwiched samples) is, however, beneficial in order to improve the data retention (i.e., low growth rates at low temperatures), whereas still providing high crystallization rates at high temperatures needed for a fast data transfer.

The preexponential constants listed in Table I for the sandwiched samples are larger than the one reported in Ref. 34 for Si_3N_4 capped $Ge_2Sb_2Te_5$ films. However, there are a few problems when comparing our data with those given in Ref. 34, where the data show a very large scatter and more importantly the reported preexponential constant, 43±25, is definitely inconsistent with the fit shown in Fig. 6 of Ref. 34. Also using the relevant growth parameters given in Table I of Ref. 34, a growth rate in the order of m/s is predicted within the temperature region they analyzed (i.e., ~5.8 m/s at 450 K) and this is of course impossible, whereas data in Fig. 6 of Ref. 34 show probably correct growth rates in the order of nm/s (i.e., ~6 nm/s at 450 K).

B. Nucleation properties

A nonlinear time dependence of the number of nuclei per unit area of *untransformed* material, N, is described by the following phenomenological relation[34] (for $t>$ the incubation time t_0):

$$N \propto t^{\alpha}, \tag{2}$$

where α denotes the "nucleation index."

It should be mentioned that N can be related to $(t-t_0)^{\alpha}$ in order to show that $N=0$ for $t<t_0$. However, in our case, although there exists an incubation time, including t_0 in Eq. (2), i.e., having $N \propto (t-t_0)^{\alpha}$, led to clearly less consistent analysis because of the following.

(i) The fits in N vs t plots (see, e.g., Fig. 5) could be performed very well on the basis of t^{α} and deteriorated if we performed them on the basis of $(t-t_0)^{\alpha}$, where t_0 was obtained from (linearly) extrapolating the average crystal radius versus time back to a radius of zero.

(ii) So-called Avrami plots of $\ln(-\ln(1-x))$ vs $\ln(t)$ (where x is the area fraction on the transformed material) showed data exhibiting a good linear dependence whereas $\ln(-\ln(1-x))$ vs $\ln(t-t_0)$ resulted in data showing a clearly curved dependence.

(iii) The so-called Avrami exponent n (as obtained from the Avrami plot) should be equal to $\alpha+D\beta$, with D the dimensionality of growth (which is 2 for the present thin film case) and β is the growth index (β=1 for interface-controlled growth and 0.5 for the

Downloaded 09 Feb 2007 to 129.125.25.39. Redistribution subject to AIP license or copyright, see http://jap.aip.org/jap/copyright.jsp

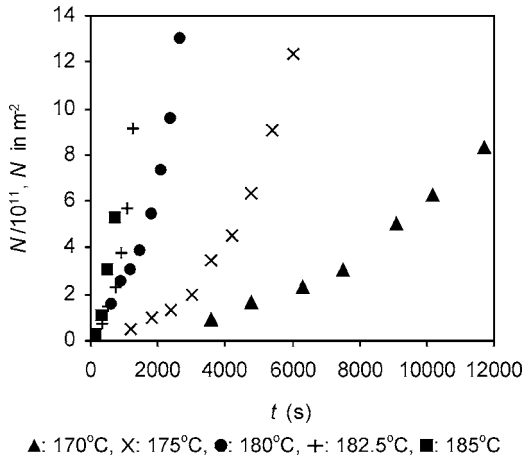

FIG. 5. Number of nuclei per unit *untransformed* area (N) as a function of time (t) during isothermal annealing of $ZnS-SiO_2$ capped Sb_xTe films at various temperatures.

diffusion-controlled growth). In the analysis excluding t_0 the equality is obeyed (within the error limits with n about 3–4, depending on the capping layer type), whereas in the analysis including t_0, n has a value of about 2, clearly inconsistent with the value of $\alpha+D\beta$.

The nucleation index α can be approximated from Eq. (2) by first calculating α_i from two consecutive images,

$$\alpha_i = \frac{\partial \ln N_i}{\partial \ln t_i} \approx \frac{\ln N_{i+1} - \ln N_i}{\ln t_{i+1} - \ln t_i}, \tag{3a}$$

and then averaging α_i as given below:

$$\alpha = \frac{\sum_i \alpha_i (1 - x_i)}{\sum_i (1 - x_i)}, \tag{3b}$$

where x_i is the area fraction of the transformed material, and it can be measured directly from the TEM images. Note that in Eq. (3b) not just a simple arithmetic average is taken but also a weighing term $(1-x_i)$ is used, since the accuracy of determined α_i is strongly decreasing when the untransformed area becomes smaller and approaches zero during the course of transformation.

N is determined by a similar procedure as proposed and used in Ref. 34. First it starts by counting the number of crystal nuclei n in a sample area A. Note that here A is not the area of a single field of view, but the sum of number of fields of view (6–10) taken into account for counting n. To convert n to N (i.e., to make it the number per unit of untransformed area) the following recursive procedure is used:

$$N_i = N_{i-1} + \frac{(n_i - n_{i-1})/A}{1 - x_{i-1}}. \tag{4}$$

This procedure is exact for infinitesimal small steps in $(1-x_i)$ and n_i. During the crystallization process, N and to lesser extent n (particularly less at the later stage of the transformation) increase with time. Figure 5 shows an example for the profound nonlinear variation of N with time during crystallization of $ZnS-SiO_2$ capped Sb_xTe films at various annealing temperatures.

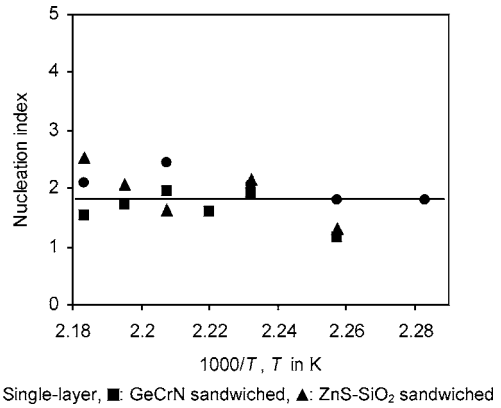

FIG. 6. Arrhenius plots of the temperature dependence of the nucleation index (α) for the three types of capped Sb_xTe films.

At each annealing temperature, by having N_i and x_i for each time step t_i, first α_i and then α are calculated using Eqs. (3a) and (3b), respectively. The nucleation index derived using the procedure outlined is shown as a function of the inverse temperature for the single-layer and sandwiched Sb_xTe films in Fig. 6. In the figure, the nucleation index does not show any detectable temperature or capping layer dependence. The average nucleation index is 1.8 ± 0.4, where the error is the standard deviation of the nucleation indices of single-layer and sandwiched Sb_xTe films. This value is significantly lower compared to that of 2.8 ± 0.6 reported for $Ge_2Sb_2Te_5$ films by Ruitenberg *et al.*[34] For a nucleation-dominant material it is probably not surprising that a higher nucleation index holds than for a fast-growth-type material, although of course the essential point is the trade-off between the nucleation and the growth rates.

The nucleation rate per unit area of the untransformed material, V_n, can be expressed as[34]

$$V_n(T) = C_n t^{\alpha-1} \exp\left(\frac{-E_n}{k_B T}\right), \tag{5}$$

where E_n is the activation energy for nucleation and C_n is a preexponential constant with respect to temperature and time. By counting the number of nuclei n on a screen area A as a function of time, the nucleation rate per unit area is determined for each isothermal annealing process using the following equation:

$$V_n = \frac{dN}{dt} = \frac{dn}{dt}\frac{1}{A(1-x)}. \tag{6}$$

Referring to Eq. (5), plotting $\ln(V_n t^{1-\alpha})$ against the reciprocal temperature $(1/T)$ yields a straight line. The slope and intercept of the line correspond to the activation energy for nucleation and preexponential constant, respectively. Figure 7 shows $\ln(V_n t^{1-\alpha})$ vs $1/T$ plots for the single-layer and sandwiched Sb_xTe films. The comparison made in Fig. 7 indicates that the nucleation rate is accelerated ~1.7 times and decelerated ~5 times when the film is sandwiched between GeCrN and $ZnS-SiO_2$ layers, respectively. Thus, the nucleation rate of the Sb_xTe film is significantly dependent

Downloaded 09 Feb 2007 to 129.125.25.39. Redistribution subject to AIP license or copyright, see http://jap.aip.org/jap/copyright.jsp

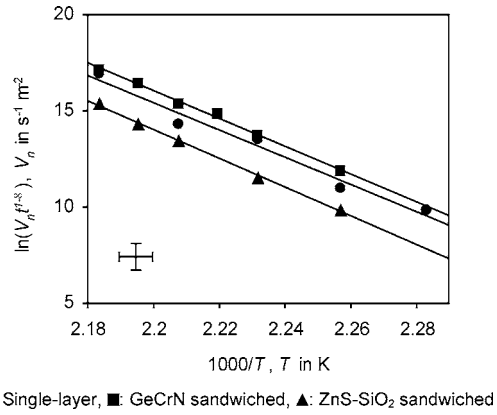

FIG. 7. Arrhenius plots of the temperature dependence of the nucleation rate (V_n) for the three types of capped Sb_xTe films.

on the capping layer type. From an application point of view, the influence of the capping layer effect on the nucleation rate can be useful, because the nucleation rate of the recording layer can be controlled by using proper capping layers. Such a control of nucleation is important for fast-growth materials to show a nucleation-free characteristic with advantages of low jitter and high amorphous phase stability.

The nucleation parameters, E_n and $\ln(C_n)$, determined for the single-layer and sandwiched Sb_xTe films are listed in Table II. $E_n=6.1\pm0.4$ eV and $\ln(C_n)=171\pm10$ for the single-layer film and these values are not strongly altered by sandwiching the film between GeCrN or $ZnS-SiO_2$ layers. Comparing these nucleation parameters with those reported for the nucleation-dominant $Ge_2Sb_2Te_5$ films in Ref. 34 is not fruitful. The reason is that the reported activation energy for nucleation (4.7 ± 1.1 eV) and the natural logarithm of the preexponential constant (166 ± 43) in Ref. 34 are too high compared to those estimated from the fit shown in Fig. 5 of Ref. 34. Another *in situ* TEM study[40] reports an activation energy for nucleation of 2.8 ± 0.3 eV for a 50 nm thick $Ge_2Sb_2Te_5$ film on a SiO_2 layer. On the basis of *ex situ* AFM measurements activation energies for the steady-state nucleation rate of 3.50 ± 0.17 and 4.09 ± 0.20 eV were obtained for 30 nm thick uncapped $Ge_2Sb_2Te_5$ and $Ge_4Sb_1Te_5$ films, respectively.[41] All these results show that the activation energy for nucleation is clearly smaller for the nucleation-dominant material than for the fast-growth material we studied.

IV. DISCUSSION

A. Why do the capping layers affect the growth rate?

In our previous report,[37] we explained the influence of the adjacent dielectric layers on the crystal growth rate in the phase-change film on the basis of the following equation:

TABLE II. Nucleation parameters E_n and $\ln(C_n)$ for the single-layer and sandwiched Sb_xTe films.

Sample	E_n (eV)	$\ln(C_n)$; C_n in $s^{-\alpha}\,m^{-2}$
Single-layer	6.1 ± 0.4	171 ± 10
GeCrN sandwiched	6.2 ± 0.2	174 ± 5
$ZnS-SiO_2$ sandwiched	6.4 ± 0.2	178 ± 4

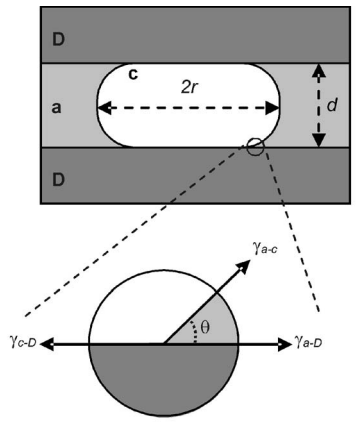

D: Dielectric layer, a: Amorphous phase-change layer,

c: Growing crystallite, *d*: Thickness of the phase-change layer,

r: Radius of the crystallite

FIG. 8. Representations of the amorphous-crystalline interface during a steady-state growth, its wetting angle (θ) with the adjacent dielectric layer, and the three interfacial energies $\gamma_{a\text{-}D}$, $\gamma_{a\text{-}c}$, and $\gamma_{c\text{-}D}$.

$$V_g = C_g \exp\left(-\frac{E_g}{kT}\right)\left[1-\exp\left(\frac{\Delta G}{kT}\right)\right]. \tag{7}$$

Equation (7) can be derived at the atomic scale where two atomic positions on both sides of an interface are considered with a Gibbs free energy difference ΔG ($\Delta G<0$). E_g is an activation energy required for an atom to jump across the interface and C_g is equivalent to an attempt frequency (ν) times jump distance (d). Then, it makes a substantial difference if these atomic positions are considered at the amorphous-crystalline (a-c) interface near the middle of the phase-change film or at the a-c interface in contact with the dielectric layers. The thinner the phase-change film the larger the fraction of atomic positions influenced by the dielectric layers and the stronger the influence of the dielectric layers on the crystal growth rate. The 20 nm phase-change film we analyzed are about 60–70 atoms thick.

Figure 8 shows various interfaces associated with the crystallite growing in a sandwiched amorphous phase-change layer. In general, the interfacial energy of an amorphous-amorphous interface is lower than that of an amorphous-crystalline one ($\gamma_{a\text{-}c}$), and therefore it is possible that the amorphous dielectric layers do not want crystallization to occur, because the amorphous-dielectric interface energy ($\gamma_{a\text{-}D}$) is less than the crystalline-dielectric interface energy ($\gamma_{c\text{-}D}$). This consideration is consistent with our observation that both ZSO and GCN capping reduces the growth rate. Simultaneously, it does not have to imply that the nucleation rate is reduced by the capping layers, because if $\gamma_{c\text{-}D}<\gamma_{a\text{-}c}$ nucleation can still be accelerated by the capping layer as is maybe the case with GCN, whereas for ZSO then $\gamma_{c\text{-}D}<\gamma_{a\text{-}c}$ and the nucleation rate is reduced. Unfortunately, these interfacial energies are not known. However, Kalb *et al.* recently measured (a lower limit for) the crystal-melt interfacial energy for various phase-change materials including a Sb rich alloy via differential thermal analysis (DTA) based undercooling experiments.[42]

Downloaded 09 Feb 2007 to 129.125.25.39. Redistribution subject to AIP license or copyright, see http://jap.aip.org/jap/copyright.jsp

Note that our experiments show that the reduction in growth velocity (by the dielectric capping layers) is only dramatic at relative low temperatures, where it thus improves data retention, but it tends to disappear at relative high temperatures, where a high data transfer rate is required. In our analysis performed in Sec. III A we can incorporate this reduction in a phenomenological way in the activation energy for growth E_g. However, it is not obvious by what physical mechanism the type of dielectric layer affects the activation energy for growth that is in principle an intrinsic property of the *a-c* interface within the phase-change film. On the other hand, the effect on ΔG is obvious because, when considering ΔG on a global scale, it is the sum of the bulk, interface, and strain energy terms. Neglecting the strain energy term (more on this in Sec. IV B), ΔG is then

$$\Delta G = (G_c - G_a)\pi r^2 d + \gamma_{c\text{-}a} 2\pi r d + (\gamma_{c\text{-}D} - \gamma_{a\text{-}D})\pi r^2, \quad (8)$$

where G_c and G_a are the bulk energies of the crystalline and amorphous phases, respectively. r is the crystal radius and d is the phase-change film thickness (i.e., 20 nm). As expected, the last term involving the film-dielectric interfacial energy becomes more important the thinner the phase-change film. At the melting temperature (T_m), $G_c - G_a$ is zero and its value becomes increasingly more negative at lower temperatures. Our measurements are performed at relative low temperatures just above the glass transition temperature T_g and well below T_m. Therefore, it can be expected that ΔG is not small and also not strongly changing within the temperature interval of our measurements. Hence, the last term in Eq. (7) can explain a 10% constant reduction in growth rate, but cannot explain the strong (up to a factor of 7) reduction, that is also strongly varying with temperature, as we observe.

A more plausible physical origin for the large variations in $C_g \exp(-E_g/kT)$ we observe can be the viscosity of the phase-change material, which is often taken according to the Stokes-Einstein relation directly proportional with the reciprocal of the jump attempt frequency $1/\nu$.[43–45] In some cases the viscosity is described by an Arrhenian temperature dependence.[45–48] However, in most cases the (strongly temperature dependent) Vogel-Fulcher-Tammann (VFT) relation (that holds particularly in the, for us correct, temperature range $T_g < T < T_g + 100$ K) is used to describe the viscosity η,[42,49–52]

$$\eta(T) = \eta_0 \exp\left(\frac{A}{T - T_0}\right), \quad (9)$$

where η_0 and A are constants. T_0 is the ideal glass transition temperature that universally is about $T_g - 50$ K. Again, the viscosity is in principle an intrinsic property of the phase-change material. Nevertheless, it is likely that the viscosity within a certain phase is largely influenced if this phase is strongly confined at the nanometer scale by more or less rigid walls. Such a confinement should in general result in an increase in viscosity (i.e., atomic rearrangements are limited), leading to a reduction in growth rate. This is in accordance with our observations that adding capping layers to the phase-change film reduces the growth rate. If the capping layers cause, for instance, a small variation in A or T_0 in the VFT relation, its effect will be most pronounced near T_g and will decrease at higher temperatures and can thus explain our observation that the reduction in growth rate by the capping layers is most pronounced at the lowest temperatures.

B. How do the capping layers affect the overall crystallization rate?

In fact, crystallization is a two-step process involving nucleation and subsequent growth of critical nuclei. In actual applications of fast-growth-type phase-change materials nucleation is in principle not required at all, since crystallization (i.e., erasing) of an amorphous written mark proceeds by growth from the crystalline rim to the center of the mark without requiring any crystal nucleation. Moreover, very low nucleation rates are beneficial for having a good archival stability and a low jitter level. When the phase-change layer is sandwiched, both the nucleation and growth processes are in principle dominated by (i) the phase-change capping layer interfaces when the phase-change layer is very thin and (ii) the bulk when the phase-change layer is thick. The interfacial effect of the capping layers can be attributed to factors such as interface morphology, stress at the interface interfacial energy, and according to the previous section "interfacial confinement."

Since the crystals nucleate at the interface,[27,34,53] the interface morphology is expected to have some influence on nucleation. However, it has been shown that the morphology does not play a vital role in the crystallization[25] although it can differ due to different types of capping layers and/or different deposition procedures. Considering the second factor, capping layers can induce either tensile or compressive stress within the phase-change layer at the interface depending on their material type. These induced stresses should then affect the crystallization temperatures, i.e., tensile and compressive stresses should correspond to higher and lower crystallization temperatures, respectively.[27,28] However, it is reported[25] that the magnitudes of these stresses are low (~80 MPa) and do not differ significantly with capping layer type. In another work[28] both tensile (200 MPa) and compressive (250–400 MPa) stresses were measured for different types of capping layers, but in all cases the crystallization temperature went up, indicating that the stresses (of these magnitudes) do not play an important role in crystallization. Thus, in principle only the third and fourth factors, i.e., a kind of "pure" interfacial energy that is only based on (chemical/physical) bonding states at the interface or the interfacial confinement, remain as origin for the difference in the crystallization, where the role of the interfacial energy has already been emphasized by a few authors.[25,28,53]

Ohshima[25] studied the influence of various dielectric protective layers (including ZnS–20 mol % SiO_2) on the crystallization process of $Ge_1Sb_2Te_4$ film. He reported that the activation energy for total crystallization of the single-layer film is 2.2 eV and it increases up to 3 eV (for SiO_2) when the capping layers are included. Since the activation energy as used by Ohshima is the activation energy for total crystallization, which includes both the nucleation and growth processes, a direct comparison between our E_g (or E_n) and the above mentioned activation energy cannot be

Downloaded 09 Feb 2007 to 129.125.25.39. Redistribution subject to AIP license or copyright, see http://jap.aip.org/jap/copyright.jsp

made. However, the total activation energy (Q) can be calculated for our samples by having E_g and E_n using the following equation:

$$Q = \frac{E_n + D\beta E_g}{\alpha + D\beta}, \tag{10}$$

where D is the dimensionality of growth ($D=1$, 2, and 3 for one-dimensional, two-dimensional, and three-dimensional growths, respectively) and β is the growth index ($\beta=1$ for interface-controlled growth and 0.5 for the diffusion-controlled growth). For our case $D=2$ and $\beta=1$. The calculated Q values are 2.9±0.3, 3.4±0.2, and 3.5±0.4 for the single-layer, GeCrN, and $ZnS-SiO_2$ sandwiched Sb_xTe films, respectively. Note that, in fact, Q is (generally) close to the corresponding E_g.

It has been shown earlier that sandwiching the nucleation-dominant films such as $Ge_1Sb_2Te_4$ and $Ge_2Sb_2Te_5$ with $ZnS-SiO_2$ layers leads to an increase of 0.4–0.5 eV in Q.[25,32] Almost a similar increase of 0.5–0.6 eV in Q is found in our case for Sb_xTe films. However, from the present measurements it is clear that this increase is caused by the increase in the activation energy for crystal growth and not by the one for nucleation. Njoroge *et al.*[28] determined a Q of 3.03±0.17 eV for an uncapped $Ag_5In_6Sb_{59}Te_{30}$ film and they found that this value increases to 3.24±0.12 eV and decreases to 2.39±0.10 eV when the film is sandwiched between Si_3N_4 and $ZnS-SiO_2$ layers, respectively. The reduction in Q they found for $ZnS-SiO_2$ sandwiching contrasts with our results and also the results of both Refs. 25 and 32, where $ZnS-SiO_2$ sandwiching leads to an increase in Q. The capping layer influence on the nucleation rate observed in the present investigation has also another interesting similarity with Ohshima's work.[25] He reported (for $Ge_1Sb_2Te_4$ films) that the nucleation is accelerated by Si_3N_4, whereas it is retarded by SiO_2 capping layers. In our case (for Sb_xTe films), we find that the nucleation is accelerated by GeCrN and it is decelerated by $ZnS-SiO_2$ capping layers.

V. CONCLUSIONS

The influence of two types of capping layers, GeCrN and $ZnS-SiO_2$, on the isothermal crystallization process of doped Sb_xTe films was analyzed using transmission electron microscopy. Direct and quantitative information on both nucleation and growth was obtained, whereas previous studies only analyzed the overall crystallization. The temperature-dependent crystal growth rate reduces if the phase-change film is sandwiched between the amorphous dielectric layers and turns out to be dependent on the capping layer type. The effect of capping layers on the growth rate is pronounced at lower temperatures ~160 °C and it tends to disappear at higher temperatures ~200 °C. The activation energy for crystal growth is 2.4±0.3 eV for the single-layer film and it increases by ~40 % when the capping layers, GeCrN or $ZnS-SiO_2$, are added. The nucleation rate shows temperature and time dependence. The "nucleation index" is found to be independent of temperature and the capping layer type. It is determined as 1.8±0.4. GeCrN layers accelerate the nucleation by a factor of ~1.7, whereas $ZnS-SiO_2$ layers decelerate it ~5 times. The activation energy for crystal nucleation is almost unaffected by the capping layers and is ~6.2 eV for all the films. The variations observed in both the growth and nucleation parameters are attributed to the interfacial energy (chemical bonding) between the phase-change and capping layer materials and to the confinement of the phase-change material by the capping layer where we anticipate that it increases the viscosity within the phase-change film.

[1] S. R. Ovshinsky, Phys. Rev. Lett. **21**, 1450 (1968).
[2] K. Nakayama, K. Kojima, F. Hayakawa, Y. Imai, A. Kitagawa, and M. Suzuki, Jpn. J. Appl. Phys., Part 1 **39**, 6157 (2000).
[3] S. Lai and T. Lowrey, Tech. Dig. - Int. Electron Devices Meet. **2001**, 803.
[4] J. Maimon, K. Hunt, J. Rodgers,L. Burcin, and K. Knowles, Proceedings of the Non-Volatile Memory Technology Symposium, 2002 (unpublished), Paper No. 23, see http://www.ovonyx.com/nvmtx_11_02.pdf
[5] M. Gill, T. Lowrey, and J. Park, Proceedings of the 2002 IEEE International Solid-State Circuits Conference, Digest of Technical Papers 2002 Paper No. 12.4, p. 158.
[6] K. Nakayama *et al.*, Jpn. J. Appl. Phys., Part 1 **42**, 404 (2003).
[7] F. Pellizzer *et al.*,Proceedings of the 2004 IEEE Symposium on VLSI Technology, Digest of Technical Papers, 2004, Paper No. 3.1, p. 18.
[8] V. Giraud, J. Cluzel, V. Sousa, A. Jacquot, A. Dauscher, B. Lenoir, H. Scherrer, and S. Romer, J. Appl. Phys. **98**, 013520 (2005).
[9] F. Yeung *et al.*, Jpn. J. Appl. Phys., Part 1 **44**, 2691 (2005).
[10] H.-Y. Cheng, C. A. Jong, R.-J. Chung, T.-S. Chin, and R.-T. Huang, Semicond. Sci. Technol. **20**, 1111 (2005).
[11] M. Chen, K. A. Rubin, and R. W. Barton, Appl. Phys. Lett. **49**, 502 (1986).
[12] G.-F. Zhou, Mater. Sci. Eng., A **304**, 73 (2001).
[13] H. Borg, M. Lankhorst, E. Meinders, and W. Leibbrandt, Mater. Res. Soc. Symp. Proc. **674**, V.1.2.1 (2001).
[14] T.-Y. Lee and K.-B. Kim, Appl. Phys. Lett. **80**, 3313 (2002).
[15] H. J. Borg, M. van Schijndel, J. C. N. Rijpers, M. H. R. Lankhorst, G. Zhou, M. J. Dekker, I. P. D. Ubbens, and M. Kuijper, Jpn. J. Appl. Phys., Part 1 **40**, 1592 (2001).
[16] N. Oomachi, S. Ashida, N. Nakamura, K. Yusu, and K. Ichihara, Jpn. J. Appl. Phys., Part 1 **41**, 1695 (2002).
[17] P. K. Khulbe, T. Hurst, M. Horie, and M. Mansuripur, Appl. Opt. **41**, 6220 (2002).
[18] Y.-C. Her and Y.-S. Hsu, Jpn. J. Appl. Phys., Part 1 **42**, 804 (2003).
[19] M. H. R. Lankhorst, L. van Pieterson, M. van Schijndel, B. A. J. Jacobs, and J. C. N. Rijpers, Jpn. J. Appl. Phys., Part 1 **42**, 863 (2003).
[20] Y.-C. Her, H. Chen, and Y.-S. Hsu, J. Appl. Phys. **93**, 10097 (2003).
[21] J. Hellmig, A. V. Mijiritskii, H. J. Borg, K. Musialkova, and P. Vromans, Jpn. J. Appl. Phys., Part 1 **42**, 848 (2003).
[22] D. Chang, D. Yoon, M. Ro, I. Hwang, I. Park, and D. Shin, Jpn. J. Appl. Phys., Part 1 **42**, 754 (2003).
[23] M. H. R. Lankhorst, B. W. S. M. M. Ketelaars, and R. A. M. Wolters, Nat. Mater. **4**, 347 (2005).
[24] M. Horie and T. Ohno, Thin Solid Films **278**, 74 (1996).
[25] N. Ohshima, J. Appl. Phys. **79**, 8357 (1996).
[26] G. F. Zhou, B. A. J. Jacobs, and W. van Es-Spiekman, Mater. Sci. Eng., A **226**, 1069 (1997).
[27] J. Tominaga, T. Nakano, and N. Atoda, Jpn. J. Appl. Phys., Part 1 **37**, 1852 (1998).
[28] W. K. Njoroge, H. Dieker, and M. Wuttig, J. Appl. Phys. **96**, 2624 (2004).
[29] N. Yamada, E. Ohno, K. Nishiuchi, N. Akahira, and M. Takao, J. Appl. Phys. **69**, 2849 (1991).
[30] N. Ohshima, J. Appl. Phys. **83**, 5244 (1998).
[31] T. H. Jeong, M. R. Kim, H. Seo, S. J. Kim, and S. Y. Kim, J. Appl. Phys. **86**, 774 (1999).
[32] I. Friedrich, V. Weidenhof, W. Njoroge, P. Franz, and M. Wuttig, J. Appl. Phys. **87**, 4130 (2000).
[33] C. Rivera-Rodríguez, E. Prokhorov, G. Trapaga, E. Morales-Sánchez, M. Hernandez-Landaverde, Y. Kovalenko, and J. González-Hernández, J. Appl. Phys. **96**, 1040 (2004).
[34] G. Ruitenberg, A. K. Petford-Long, and R. C. Doole, J. Appl. Phys. **92**, 3116 (2002).
[35] B. J. Kooi, W. M. G. Groot, and J. Th. M. De Hosson, J. Appl. Phys. **95**,

Downloaded 09 Feb 2007 to 129.125.25.39. Redistribution subject to AIP license or copyright, see http://jap.aip.org/jap/copyright.jsp

924 (2004).
[36]B. J. Kooi and J. Th. M. De Hosson, J. Appl. Phys. **95**, 4714 (2004).
[37]B. J. Kooi, R. Pandian, J. Th. M. De Hosson, and A. Pauza, J. Mater. Res. **20**, 1825 (2005).
[38]R. Pandian, B. J. Kooi, J. Th. M. De Hosson, and A. Pauza (unpublished).
[39]J. Kalb, F. Spaepen, and M. Wuttig, Appl. Phys. Lett. **84**, 5240 (2004).
[40]S. Privitera, C. Bongiorno, E. Rimini, R. Zonca, A. Pirovano, and R. Bez, Mater. Res. Soc. Symp. Proc. **803**, HH1.4.1 (2004).
[41]J. A. Kalb, C. Y. Wen, F. Spaepen, H. Dieker, and M. Wuttig, J. Appl. Phys. **98**, 054902 (2005).
[42]J. A. Kalb, F. Spaepen, and M. Wuttig, J. Appl. Phys. **98**, 054910 (2005).
[43]D. R. Uhlmann, J. Non-Cryst. Solids **7**, 337 (1972).
[44]B. Hyot, L. Poupinet, V. Gehanno, and P. J. Desre, J. Magn. Magn. Mater. **249**, 504 (2002).
[45]S. Senkader and C. D. Wright, J. Appl. Phys. **95**, 504 (2004).
[46]I. Avramov, Ts. Vassilev, and I. Penkov, J. Non-Cryst. Solids **351**, 472 (2005).
[47]J. Kalb, F. Spaepen, T. P. Leervad Pedersen, and M. Wuttig, J. Appl. Phys. **94**, 4908 (2003).
[48]K. A. Sharaf, A. H. Abou El-Ela, and A.-A. El-Maboud, Fiz. A **9**, 67 (2000).
[49]M. Fontana, B. Arcondo, M. T. Clavaguera-Mora, and N. Clavaguera, Philos. Mag. B **80**, 1833 (2000).
[50]J. Rault, J. Non-Cryst. Solids **271**, 177 (2000).
[51]B. Hyot, L. Poupinet, J. Marty, X. Durand, and P. J. Desre, Proceedings of the EPCOS, 2004 (unpublished), www.epcos.org/pdf_2004/09paper_hyot.pdf
[52]I. Avramov, J. Non-Cryst. Solids **351**, 3163 (2005).
[53]H. C. F. Martens and R. Vlutters, J. Appl. Phys. **95**, 3977 (2004).

Downloaded 09 Feb 2007 to 129.125.25.39. Redistribution subject to AIP license or copyright, see http://jap.aip.org/jap/copyright.jsp